Green synthesis of ZnO nanoparticles using *Indigo era colutea* leaf extracts

S. P. Sudhakar[1], D. Prema[2], S. Velmurugan[3] and M. Kamaraj[1*]

[1]Department of Botany, Jamal Mohamed College, Tiruchirappalli, Tamil Nadu-620 020.

[2]Department of Biochemistry, Holy Cross College, Tiruchirappalli, Tamil Nadu -620 001.

[3]Department of Botany, Alagappa Government Arts College, Karaikudi-630 003.

Abstract

Zinc oxide nanoparticles (ZnO NPs) were synthesized by green method using *Indigofera colutea* leaf extracts. Synthesized nanoparticles were characterized by XRD, XPS, FESEM, TEM, EDAX, FTIR, UV-Vis and PL studies carried out. Structural and Morphology were identified by XRD, XPS, FESEM and TEM analysis. Chemical composition were demonstrated through EDAX spectra. The various function groups were identified by FT-IR spectra. Optical studies were carried out using UV and PL spectra. *Invitro* cytotoxicity effect was analysed for MCF-7 (human breast cancer cell line).

Keywords: ZnO, Nanoparticles**,** *Indigofera colutea* leaf, Breast cancer.

1. Introduction

Zinc oxide nanoparticles is one of the important semiconductor materials for wide band gap 3.36 eV and large exciton binding energy 60 meV at room temperature. This makes us interesting for its electro-optical applications [1]. The metal oxide nanomaterials are attractive for use in biomedical applications. It has been proposed that the high surface area of metal oxide nanoparticles significantly enhances their ability to produce reactive oxygen species (ROS) [2,3]. Toxicity of ZnO NPs is reported due to the generation of intracellular ROS and release of Zn^{2+} ions [4]. ROS is generated through various mechanisms such as illumination of nanomaterials by ultraviolet (UV) light, disturbance of intracellular metabolic activities, and antioxidant system, result in the generation of oxidative stress in the cells. ROS can damage DNA, cell membrane, and proteins which may lead to cell death [5,6]. *Indigofera colutea* (*Burm.f.) Merr.* is a plant accepted name of a species in the genus Indigofera (family *Leguminosae*).

In present work, ZnO NPs are synthesized by green method using *Indigofera colutea* leaf extract. We have studied the structural, morphological, optical and anticancer properties of ZnO NPs. The green-synthesis of ZnO NPs were characterization done by UV-Visible, XRD, XPS, FESEM, EDAX TEM, FT-IR, UV-Vis, Photoluminescence and anticancer activity analyses.

2 Materials and Methods

2.1 Green synthesis of ZnO NPs

Fresh *Indigofera colutea* leaves were collected from Tiruchirappalli (Tamil Nadu, India) and used to retrieve their extraction. First, the leaves were cleaned with tap water, followed by distilled water and then finely cut into small pieces. Ten grams of finely cut leaves was added with 100 mL of double distilled water and boiled at 80°C for 10 min. The obtained extraction was filtered using Whatman No. 1 filter paper. Then, 0.1 M Zn $(NO_3)_2$. $6H_2O$ solution was dissolved into 150 ml of *Indigofera colutea* leaf extract. Homogenously Zinc nitrate solution was continuously stirred at 80 ^oC for 6h. The yellow colour precipitate was obtained. Further the precipitate was dried at 120 ^oC for 2h. The obtained ZnO nanopowder were annealed at 700 ^oC for 5h.

2.2 Cell Viability Assay

MTT assay was carried out as described previously. *Indigofera colutea* leaf extracts capped ZnO NPs, in the concentration range 10-100 µg/ml concentration of ZnO NPs was added to the wells 24 h after seeding of 5 x 10^3 cells $well^{-1}$ in 200 µL of a fresh culture medium. After 24 h, 20 µL of a MTT solution [5 mg/mL in phosphate-buffered saline (PBS)] was added to each well, and the plates were wrapped with aluminum foil and incubated for 4 h at 37 ˚C. The purple formazan product was dissolved by the addition of 100 µL of DMSO to each well. Spectrophotometrical absorbance of the purple blue formazan dye was measured in a microplate reader at 570 nm (Biorad 680). Cytotoxicity was determined using Graph pad prism 5 software. The percentage inhibition was calculated, from this data, using the formula

= (mean OD of untreated cells (control) – mean OD of treated cells / mean OD of untreated cells) x 100.

2.3 Characterization Techniques

The ZnO NPs was characterized by X-ray diffractometer (model: X'PERT PRO PANalytical). The diffraction patterns were recorded in the range of 30º-80º for the ZnO NPs samples where the monochromatic

wavelength of 1.54 Å was used. The XPS measurements were performed with XPS instrument (Carl Zeiss) equipment. The spectra were at a pressure using ultra high vacuum with Al Kα excitation at 250 W. The samples were analyzed by Field Emission Scanning Electron Microscopy (Carl Zeiss Ultra 55 FESEM) with EDAX (model: Inca). The morphology of the synthesized ZnO was examined using TEM. Samples for TEM analysis were prepared by drop coating the nanoparticles solutions on carbon-coated copper grids at room temperature. The excess nanoparticles solution was removed with filter paper. The copper grid was finally dried at room temperature and was subjected to TEM analysis by the instrument Tecnai F20 model operated at an accelerating voltage of 200 kV. The FT-IR spectra were recorded in the range of 400-4000 cm^{-1} by using Perkin-Elmer spectrometer. The absorption spectra of ZnO NPs were studied in the range between 200 and 1100 nm by Lambda 35 spectrometer. Photoluminescence spectra were taken using spectrometer Perkin Elmer-LS 14.

3 Results and Discussion

3.1 X-ray diffraction studies

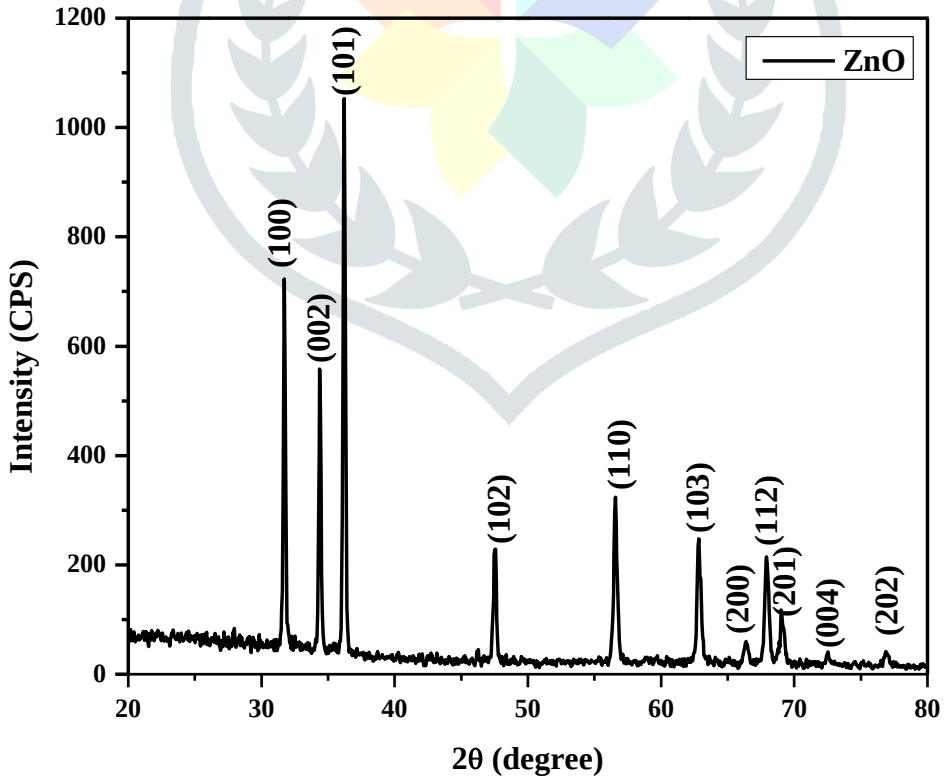

Figure 1 XRD pattern of green synthesized ZnO NPs using *Indigofera colutea* leaf extract.

The XRD pattern of the green synthesized ZnO NPs using *Indigofera colutea* leaf extract is shown in Fig. 1. The XRD peaks are appeared at angles (2θ) of 32.812˚, 34.336˚ and 36.269˚ corresponding to (100), (002) and (101) planes of ZnO NPs. Similarly, other peaks found at angles (2θ) of 47.576, 56.605, 62.865, 66.35, 67.91, 69.12, 72.48 and 76.82 are corresponding to (102), (110), (103), (200), (112), (201), (004) and (202) planes of ZnO NPs exhibits hexagonal wurtzite structure with space group of p63mc. Which is also confirmed by the (JCPDS card No: 79-2205) values are given in Table 1. The average crystallite size of the ZnO NPs was estimated using Debye Scherrer's relation.

$$\text{Average crystallite size (D)} = \frac{0.9\,\lambda}{\beta \cos\theta}$$

Where, λ is the wave length of X-ray used (1.54060 Å), β is the angular peak width at half maximum in radians and θ is Bragg's diffraction angle. The average crystallite size is calculated as 47.20 nm for ZnO NPs.

Table 1 As compared ZnO NPs and JCPDS data values.

JCPDS Card no: (79-2205) 2θ (degree)	ZnO 2θ (degree)	JCPDS Card no: (79-2205) d-spacing [Å]	ZnO d-spacing [Å]	JCPDS Card no: (79-2205) FWHM β (˚)	ZnO 2θ FWHM β (˚)	(hkl)	JCPDS Card no: (79-2205) Relative Intensity	ZnO Relative Intensity
31.799	31.7251	2.8146	2.82053	0.228	0.1968	(100)	56.40	65.62
34.419	34.3805	2.6035	2.60852	0.21	0.1968	(002)	41.50	50.71
36.251	36.2160	2.4760	2.48042	0.237	0.1968	(101)	99.99	100.00
47.536	47.5426	1.9112	1.91258	0.35	0.2460	(102)	21.10	20.10
56.591	56.5589	1.6250	1.62723	0.29	0.2460	(110)	30.50	29.61
62.851	62.7905	1.4773	1.47990	0.42	0.3444	(103)	26.80	22.08
66.371	66.3892	1.4073	1.40814	0.4	0.2952	(200)	4.00	4.04
67.942	67.8952	1.3785	1.38053	0.36	0.3444	(112)	21.70	19.34
69.081	69.0568	1.3585	1.36012	0.42	0.1968	(201)	10.6	9.21
76.953	72.4901	1.2380	1.30393	0.7	0.2952	(202)	3.30	1.97

3.2 XPS studies

XPS spectra of green synthesized ZnO NPs using *Indigofera colutea* leaf extract is shown in Fig. 2. The Zn (2p) and O (1s) oxidation states were identified using XPS spectra. The Zn (2p) state split in two doublets, such as Zn $2p_{1/2}$ and Zn $2p_{3/2}$ observed at 1021.98 and 1044.19 eV respectively, is attributed Zn^{2+} bound to oxygen in the ZnO matrix [7]. Figure 3 shows the O (1s) oxidation state split in two signal observed at 530.30 and 532.49 eV

respectively. The first binding energy O (1s) signal centre at 530.30 eV, which may be O_2^- ion in the wurtzite. The second binding energy located at 532.49 eV, due to the loosely-bound oxygen, like absorbed O_2 or adsorbed H_2O on the ZnO surface.

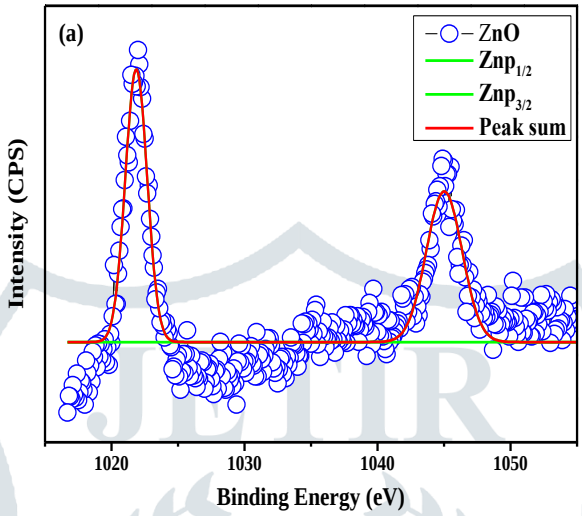

Figure 2 XPS spectra of Zn (2p) oxidation state for ZnO NPs using *Indigofera colutea* leaf extract

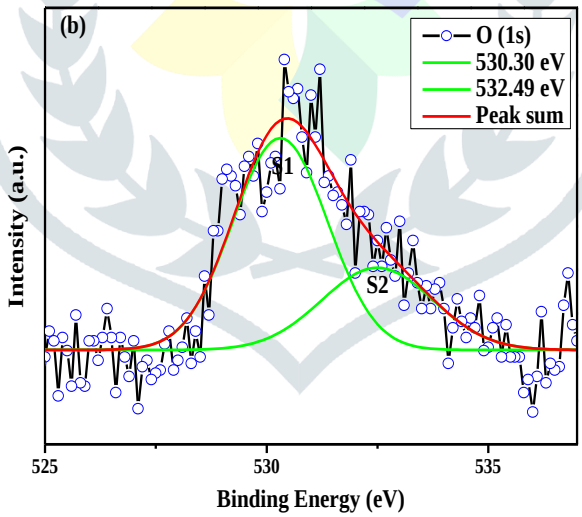

Figure 3 XPS spectra of O (1s) oxidation state for ZnO NPs using *Indigofera colutea* leaf extract

3.3 FESEM and EDAX analysis

Figure 4 (a-b) shows the FESEM images for green synthesized ZnO NPs exhibits hexagonal nanostructures and average particle size is found to be 41 nm. This is also confirmed by the XRD results. The chemical

composition of ZnO NPs is shown in Fig. 4 (c). It is evident that, the estimated elements Zn and O are found to be 47.93% and 52.07% respectively.

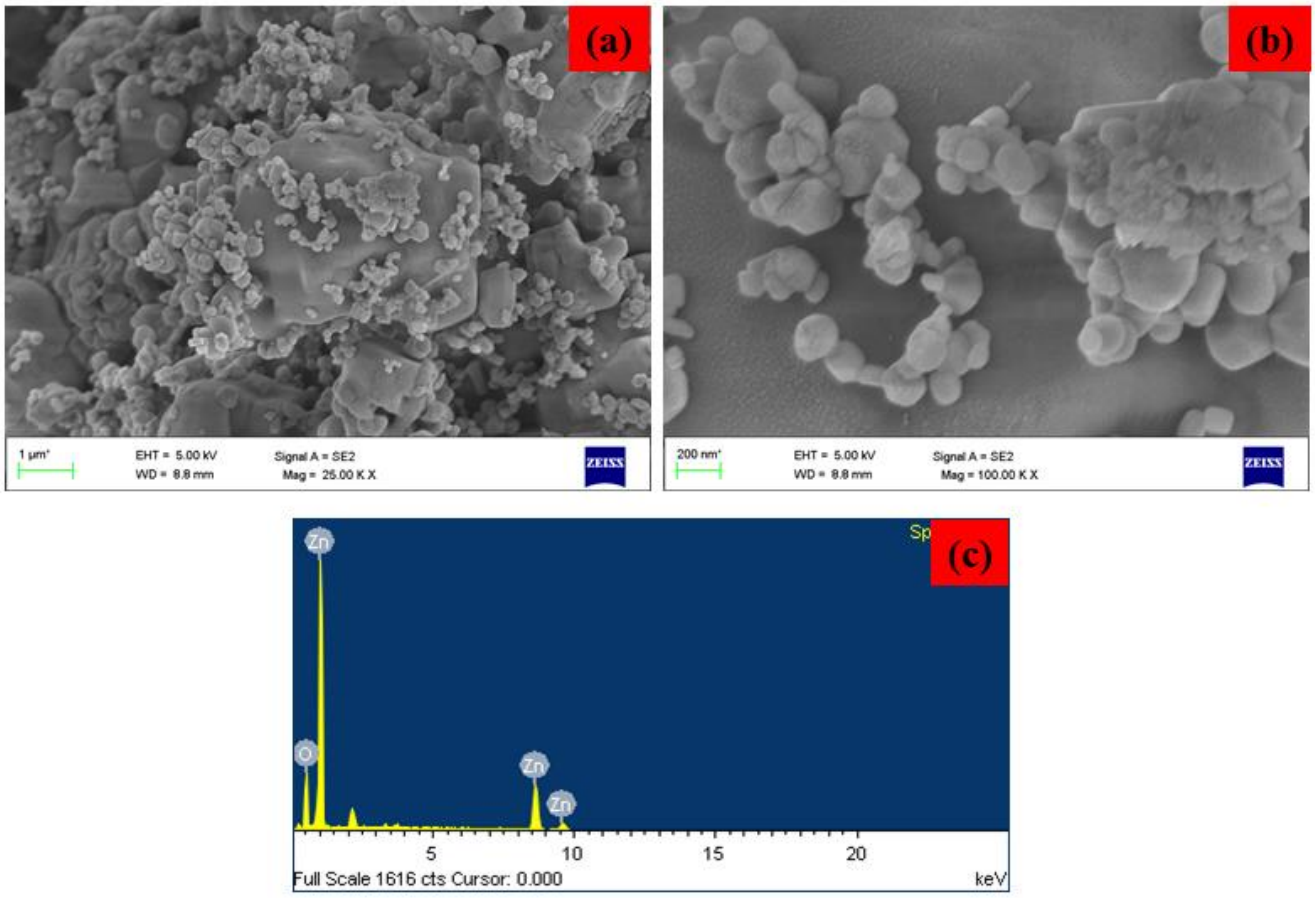

Figure 4 FE-SEM images of (a-b) ZnO NPs and EDAX spectrum of (c) ZnO NPs

3.4 High Resolution – Transmission Electron Microscopy (HR-TEM)

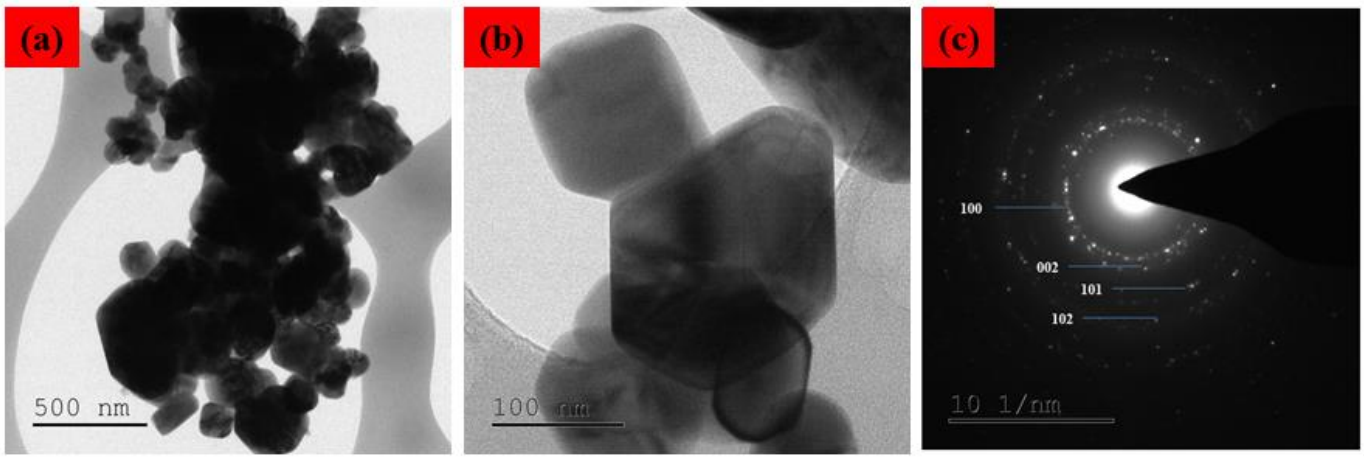

Fig. 5a & 5b: HRTEM images & Fig. 5c: SAED studies of ZnO NPs

The HRTEM images of green synthesized ZnO NPs is shown in Fig. 5a and 5b. The ZnO NPs formed a hexagonal structure and average particles size is found to be 40 nm. The crystallinity of the synthesized ZnO NPs was examined by selected area diffraction studies. Figure 5c shows the reflections (100), (002), (101), (102) and (110) of wurtzite hexagonal structure for ZnO NPs and no additional rings in the SAED pattern stemming from any crystalline impurities.

3.5 FT-IR spectroscopic studies

Figure 6 shows the FTIR spectrum of the synthesized ZnO NPs in the range of 4000–400 cm^{-1}. The broad O-H stretching and bending of water molecules observed at 3415 cm^{-1} and 1360 cm^{-1} for ZnO sample [8]. The peaks at 2989 and 2337 cm^{-1} are due to symmetric and asymmetric C–H bands [9]. The C=C stretching group observed at 1708 cm^{-1} for ZnO sample. The weak Zn–O stretching frequencies are observed at 892 cm^{-1} [10]. The Zn-O stretching bands appear at 444 cm^{-1} for green synthesized ZnO NPs.

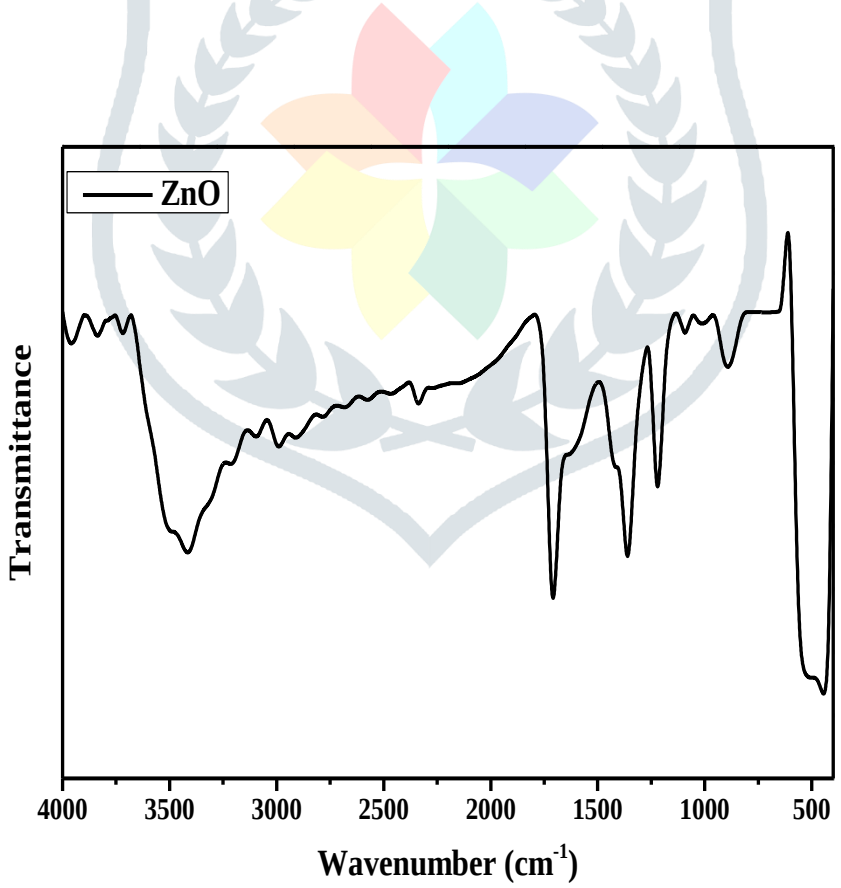

Figure 6 FTIR spectra of the ZnO NPs using *Indigofera colutea* leaf extract

3.6 UV–Vis absorption spectroscopic studies

UV-Visible optical absorption spectra were recorded at room temperature in the wavelength range 200-800 nm and shown in Fig.7. From the absorption spectra, the absorption edge peak is observed 367 nm for ZnO NPs. The optical energy band gap of ZnO NPs is calculated by classical Tauc relation as given below $\alpha h\upsilon = A (h\upsilon - E_g)^n$ [11,12]. A plot between $(\alpha h\upsilon)^2$ versus photon energy (eV) is drawn for ZnO NPs (Fig. 8). The band gap energy values of 3.1 eV is obtained for ZnO NPs.

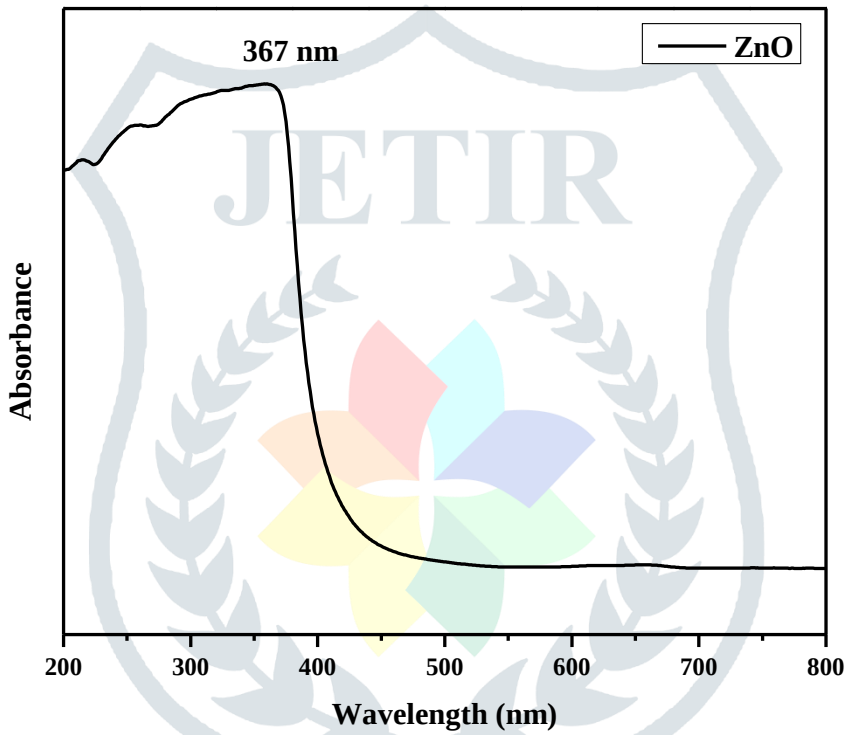

Figure 7 UV-vis spectrum of the ZnO NPs using *Indigofera colutea* leaf extract

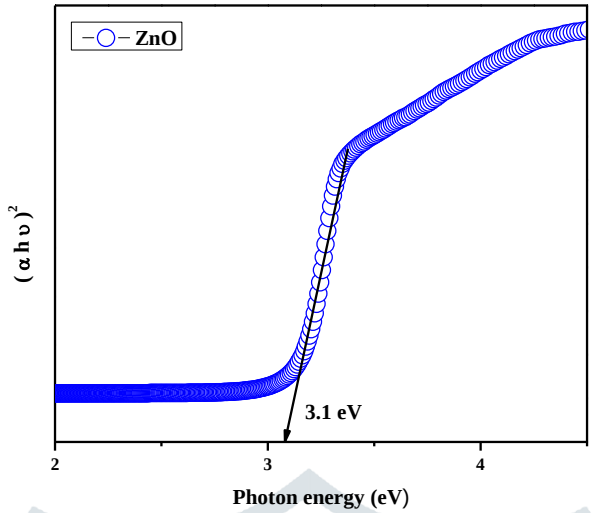

Figure 8 Tauc plots of $(\alpha h\nu)^2$ versus hν of the ZnO NPs using *Indigofera colutea* leaf extract

3.7 Photoluminescence spectroscopic studies

Figure 9 shows the photoluminescence spectra of green synthesized ZnO NPs using an excitation wavelength of 350 nm. In the case of ZnO NPs, the emission wavelengths are observed at 360 nm, 377 nm, 392 nm, 411 nm, 444 nm, 490 nm and 520 nm respectively. Three UV emission peaks are observed at 360 nm, 377 nm and 392 nm, which correspond to the near-band emission (NBE) of ZnO NPs. The two violet emissions centered at 411 and 444 nm are ascribed to an electron transition from a shallow donor level of the natural zinc interstitials to the top level of the valence band [13]. The blue-green emission observed at 490 nm is attributed to the transition between the oxygen vacancy and interstitial oxygen [14]. Finally green emission observed at 520 nm, corresponds to the singly ionized oxygen [15, 16].

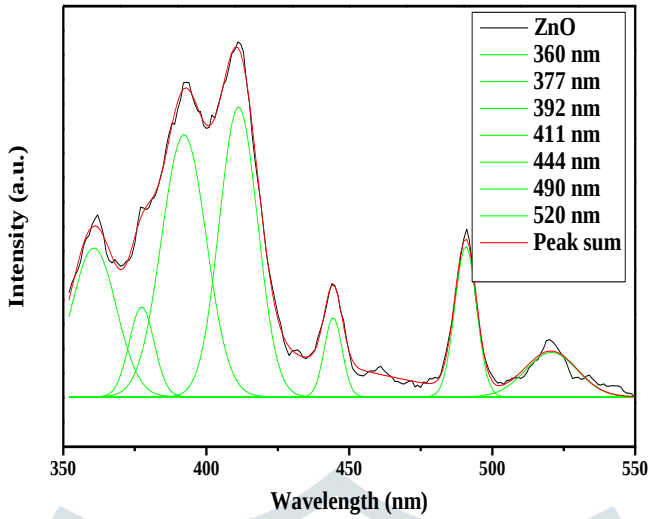

Figure 9 Gaussian de-composed photoluminescence emission spectrum of the ZnO NPs using *Indigofera colutea* leaf extract

3.8 Anticancer properties

The potential cytotoxicity of green synthesized ZnO NPs using *Indigofera colutea* leaf extract was evaluated against human breast cancer (MCF-7 cells) with different concentrations (10 to 100 µg/ml). The ZnO NPs results exhibits with dose dependent manner. The IC_{50} value of 67.70 µg/ml (evaluated after 24h) for ZnO NPs tested against MCF-7. The percentage of cell death values of ZnO is presented in Fig. 10. Cell morphological changes were observed for light microscope with different concentrations 10, 30, 50, 70 and 100 µg/ml [Fig. 11]. The anticancer efficiency of ZnO NPs generally depends on the presence of more ROS, which is mainly attributed to the size, release of Zn^{2+} and increasing oxygen vacancies [17].

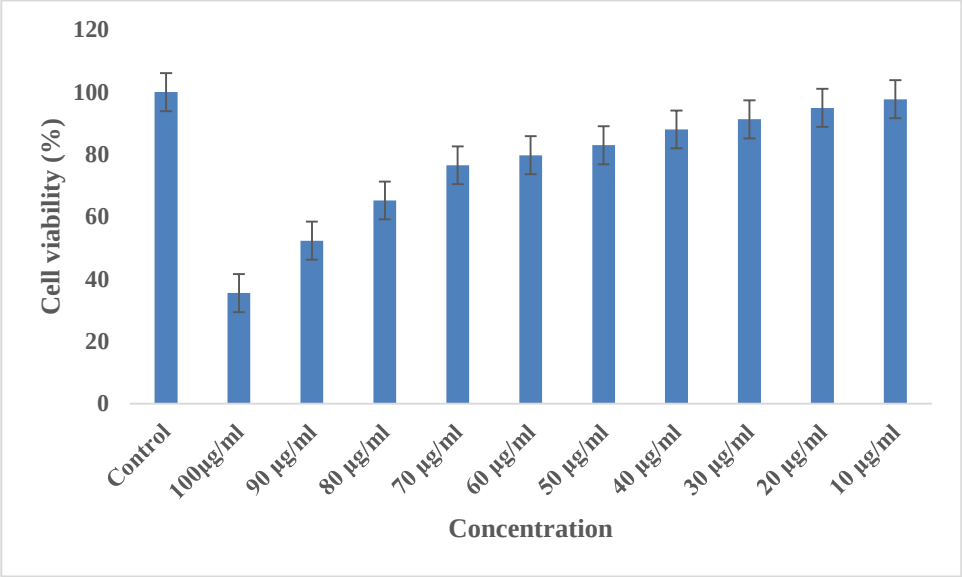

Figure 10 Cell viability was determined by a modified MTT assay using Breast cancer line (MCF-7) treated with ZnO NPs using *Indigofera colutea* leaf extract

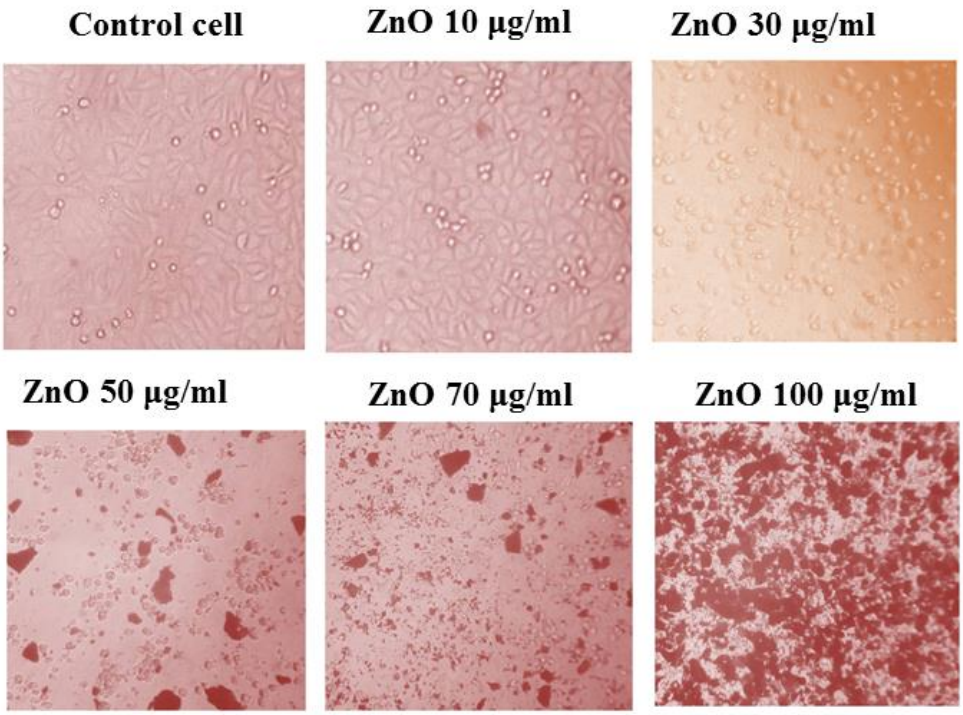

Figure 11 Cell morphological changes were observed for light microscope with different concentrations 10, 30, 50, 70 and 100 µg/ml ZnO NPs using breast cancer cell line.

Conclusion

In summary, the ZnO NPs synthesized by green method using *Indigofera colutea* leaf extracts. From the XRD patterns, the prepared ZnO NPs was exhibits hexagonal wurtzite structure. XPS spectra provided the importation about oxidation state O (1s) and Zn (2p). In the case of FESEM and TEM images, the ZnO NPs were formed hexagonal structure. Chemical compositions were estimated for the prepared ZnO using EDAX spectra. The FT-IR spectra, Zn-O vibrational frequencies were observed at 444 cm^{-1}. From UV-Vis spectra, the ZnO NPs absorption edge peak and band gap were observed at 367 nm and 3.1 eV. PL spectra of the ZnO sample the band emission may be zinc vacancies, oxygen vacancies and surface defects. The cytotoxic effect of the *green synthesized* ZnO NPs was examined on cultured MCF-7 breast cancer cells by exposing cells for 24 h and 50% of cell mortality observed at 67.70 µg/ml.

References

1. Theivarasu C, Indumathi T. Effect of rare earth metal ion Ce3+ on the structural, optical and magnetic properties of ZnO nanoparticles synthesized by the co-precipitation method. J Mater Sci Mater Electron 2016;27:1-8.
2. Møller P, Jacobsen NR, Folkmann JK, Danielsen PH, Mikkelsen L, Hemmingsen JG, et al. Role of oxidative damage in toxicity of particulates. Free Radic Res 2010;44(1):1-46.
3. Li N, Sioutas C, Cho A, Schmitz D, Misra C, Sempf J, et al. Ultrafine particulate pollutants induce oxidative stress and mitochondrial damage. Environ Health Perspect 2003;111(4):455-60.
4. Sasidharan A, Chandran P, Menon D, Raman S, Nair S, Koyakutty M. Rapid dissolution of ZnO nanocrystals in acidic cancer microenvironment leading to preferential apoptosis. Nanoscale 2011;3(9):3657-69.
5. Desnues B, Cuny C, Grégori G, Dukan S, Aguilaniu H, Nyström T. Differential oxidative damage and expression of stress defence regulons in culturable and non-culturable Escherichia coli cells. EMBO Rep 2003;4(4):400-4.
6. Aertsen A, Michiels CW. Stress and how bacteria cope with death and survival. Crit Rev Microbiol 2004;30(4):263-73.
7. Hameed, Abdulrahman Syedahamed Haja, Chandrasekaran Karthikeyan, Seemaisamy Sasikumar, Venugopal Senthil Kumar, Subramanian Kumaresan, and Ganesan Ravi. "Impact of alkaline metal ions Mg 2+, Ca 2+, Sr 2+ and Ba 2+ on the structural, optical, thermal and antibacterial properties of ZnO nanoparticles prepared by the co-precipitation method." *Journal of Materials Chemistry B* 1, no. 43 (2013): 5950-5962.

8. Nejati, Kamellia, Zolfaghar Rezvani, and Rafat Pakizevand. "Synthesis of ZnO nanoparticles and investigation of the ionic template effect on their size and shape." *International Nano Letters* 1, no. 2 (2011): 75.
9. Vorkapic, Danijela, and Themis Matsoukas. "Effect of temperature and alcohols in the preparation of titania nanoparticles from alkoxides." *Journal of the American Ceramic Society* 81, no. 11 (1998): 2815-2820.
10. Wang, X. S., Z. C. Wu, J. F. Webb, and Z. G. Liu. "Ferroelectric and dielectric properties of Li-doped ZnO thin films prepared by pulsed laser deposition." *Applied Physics A*77, no. 3-4 (2003): 561-565.
11. Liu, Mi, A. H. Kitai, and P. Mascher. "Point defects and luminescence centres in zinc oxide and zinc oxide doped with manganese." *Journal of Luminescence* 54, no. 1 (1992): 35-42.
12. Suwanboon, Sumetha, Tanattha Ratana, and Thanakorn Ratana. "Effects of Al and Mn dopant on structural and optical properties of ZnO thin film prepared by sol-gel route." *Walailak Journal of Science and Technology (WJST)* 4, no. 1 (2011): 111-121.
13. Fan, X. M., J. S. Lian, L. Zhao, and Y. H. Liu. "Single violet luminescence emitted from ZnO films obtained by oxidation of Zn film on quartz glass." *Applied surface science* 252, no. 2 (2005): 420-424.
14. Varghese, N., Panchakarla, L.S., Hanapi, M., Govindaraj, A. and Rao, C.N.R., 2007. Solvothermal synthesis of nanorods of ZnO, N-doped ZnO and CdO. *Materials Research Bulletin*, *42*(12), pp.2117-2124.
15. Kumar, Nitin, Adam Dorfman, and Jong-in Hahm. "Fabrication of optically enhanced ZnO nanorods and microrods using novel biocatalysts." *Journal of nanoscience and nanotechnology* 5, no. 11 (2005): 1915-1918.
16. Bagnall, D. M., Y. F. Chen, M. Y. Shen, Zz Zhu, T. Goto, and T. Yao. "Room temperature excitonic stimulated emission from zinc oxide epilayers grown by plasma-assisted MBE." *Journal of crystal growth* 184 (1998): 605-609.
17. Puhl, Ana Cristina, Michelle Fagundes, Karen Cristina Dos Santos, Igor Polikarpov, João Batista Fernandes, Paulo Cezar Vieira, and Moacir Rossi Forim. "Preparation and characterization of polymeric nanoparticles loaded with the flavonoid luteolin, by using factorial design." *International journal of drug delivery* 3, no. 4 (2012): 683-698.